Electronic Supporting Information

A Triple-Channel Optical Signal Probe for Hg^{2+} Detection Based on Acridine Orange and Aptamer-Wrapped Gold Nanoparticles

Wan Yi Xie, Wei Tao Huang, Jian Rong Zhang, Hong Qun Luo* and Nian Bing Li*

Key Laboratory of Eco-environments in Three Gorges Reservoir Region (Ministry of Education), School of Chemistry and Chemical Engineering, Southwest University, Chongqing 400715, P.R. China

* Corresponding authors: luohq@swu.edu.cn (H.Q. Luo) ; linb@swu.edu.cn (N.B. Li)

1. Experimental section

Chemicals and Instruments. The oigonucleotides (T10: poly-T_{10}, T15: poly-T_{15}, T20: poly-T_{20}, T35: poly-T_{35}) was prepared by Sangon Biotechnology Co., Ltd. (Shanghai, China). Single-stranded concentrations were determined by measuring the absorbance at 260 nm. Trisodium citrate and all the used metal salts, i.e. $AgNO_3$, $AlCl_3$, $BaCl_2$, $Cd(NO_3)_2$, $CoCl_2$, $CrCl_3$, $Cu(NO_3)_2$, $FeCl_3$, $MgCl_2$, $Mn(Ac)_2$, $Pb(NO_3)_2$, $ZnCl_2$, $Ni(NO_3)_2$, $NaNO_3$, and $Hg(NO_3)_2$ were of analytical grade and used as received without further purification. Stock solutions of T20 and $Hg(NO_3)_2$ were prepared in ultrapure water.

The fluorescence (FL) and resonance light scattering (RLS) spectra were measured using a Hitachi F-4500 fluorescence spectrophotometer (Hitachi Ltd., Japan) equipped with a Xenon lamp excitation source. For the FL measurements, the fluorescence spectrophotometer was set in the fluorescence mode on excitation at 490 nm and the intensity was detected at 538 nm with all excitation and emission slit widths of 10 nm. The working voltage of the PMT was 400 V. Meanwhile, for the RLS measurements, the fluorescence spectrophotometer was set in the synchronous mode with the slit widths of 5 and 5 nm for excitation and emission. The PMT voltage was set at 400 V. Ultraviolet-visible absorption spectra were recorded on Shimadzu UV-2450 spectrophotometers (Suzhou Shimadzu Instrument Co., Ltd., China). pH values were measured by a pH-3C precision pH meter (Leici Devices Factory of Shanghai, China). Transmission electron microscopy (TEM) images were obtained with a transmission electron microscope (JEM-100CXII, Japan) at a 80 KV accelerating voltage. The samples for TEM characterization were prepared by placing a drop of colloidal solution on carbon-coated copper grid and dried at room temperature.

Gold Nanoparticle Preparation: AuNPs were prepared according to the report of Turkevich.[1] Briefly, a sodium citrate solution (10 mL, 38.8 mM) was rapidly added to the boiled $HAuCl_4$ (100 mL, 1 mM) solution under vigorous stirring. The solution was heated under reflux for another 15 min, during which time its color changed from pale yellow to wine-red. The solution was cooled to room temperature while being stirred continuously. Then the prepared solution was filtered through a 0.22 μm membrane filter and stored in a refrigerator at 4 °C before being used. The surface plasma resonance (SPR) peak of the AuNPs was 520 nm, and the particle concentration of the AuNPs was 12 nM calculated according to Beer's law.[2] The average size of the AuNPs, estimated by TEM, was about 7.5 nm (Fig. S1A).

Detection of Mercury (II): The working solution of 5 μM T20 was prepared in Tris-HAc buffer solution (10 mM, pH 7.0, 100 mM $NaNO_3$), and different concentrations of Hg^{2+} were prepared in 10

mM Tris-HAc buffer solution (pH 7.0). For Hg^{2+} detection, 10 μL of the DNA probe solutions (5 μM, respectively), 10 μL of metal solution (or blank buffer solution), and 415 μL Tris-HAc buffer solution (10 mM, pH 7.0, 40 mM $NaNO_3$) was first mixed and incubated for ~20 min. Then 50 μL of AuNPs colloidal solutions as prepared were added to the mixed solution and allowed to interact for ~1 h at room temperature. After that 15 μL of 20 μM AO solution was mixed and incubated for another ~0.5 h at room temperature. In this system the aggregation of AuNPs leads to the change in the three optical signals, Thus, the operation for the FL spectra, RLS spectra and UV/vis absorption spectra can be carried out at the same time.

2. TEM images of AuNPs at different conditions

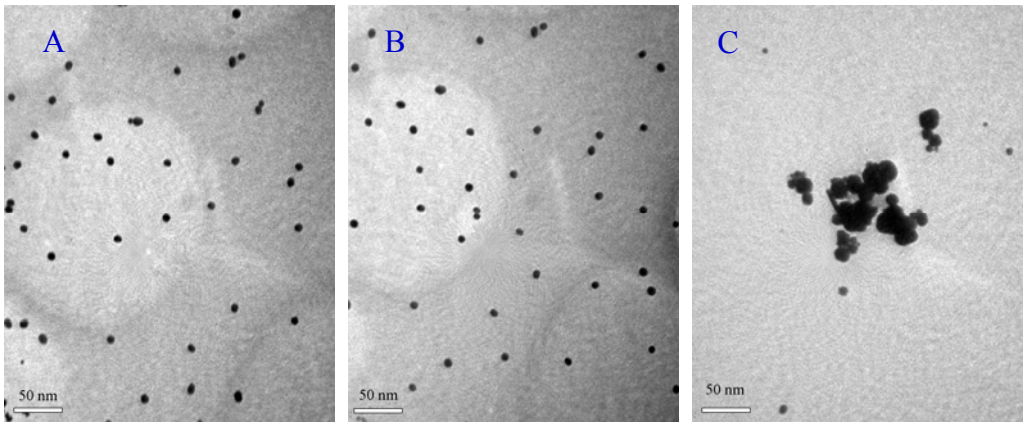

Fig. S1 TEM images of (A) AuNPs (~7.5 nm), (B) AO + T20 + AuNPs, and (C) AO + Hg^{2+} (10 μM) + T20 + AuNPs.

3. The fluorescence intensity of AO released before and after centrifugation

Fig. S2 shows the fluorescence intensity of AO/T20/AuNPs (0.6 μM/100 nM/1.2 nM) upon addition of Hg^{2+} (2 μM) before and after centrifugation (9000 r/min, 10 min). These results indicate that the fluorescence intensity of AO released before centrifugation is weaker than that after centrifugation and that the formation of dsDNA caused by Hg^{2+} is conducive to the release of AO from the surface of AuNPs.

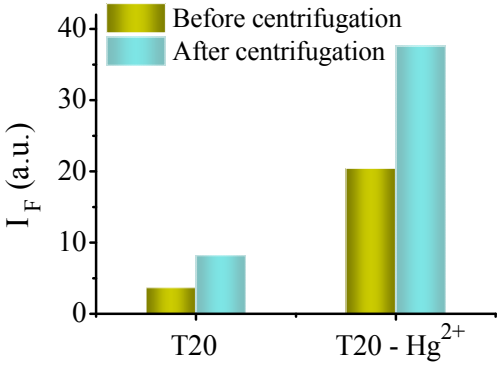

Fig. S2 The fluorescence intensity of AO/T20/AuNPs (0.6 μM/100 nM/1.2 nM) upon addition of Hg^{2+} (2 μM) before and after centrifugation. Excitation and emission wavelengths were at 490 and 538 nm, respectively.

4. Effects of AuNPs and AO concentrations

The amounts of AuNPs and AO affect the response behavior of the system for Hg^{2+}. As shown in Fig. S3, in the absence of Hg^{2+} (Fig. S3A) and in the presence of 2 μM Hg^{2+} (Fig. S3B) the fluorescence intensity of AO was increased with the addition of AO. The more the amounts of the AuNPs used, the lower the fluorescence intensity increased. At a fixed Hg^{2+} concentration of 2 μM, when the concentration of AO was low, the fluorescence of AO was easily quenched by the remaining AuNPs, which resulted in a low fluorescence signal and a small signal-to-background ratio (S/B). However, when the concentration of AO was too high, the fluorescence could not be effectively quenched by AuNPs, leading to a high background signal and thus a low S/B. Thus, 0.6 μM AO and 1.2 nM AuNPs were the optimum choices for this experiment (Fig. S3C).

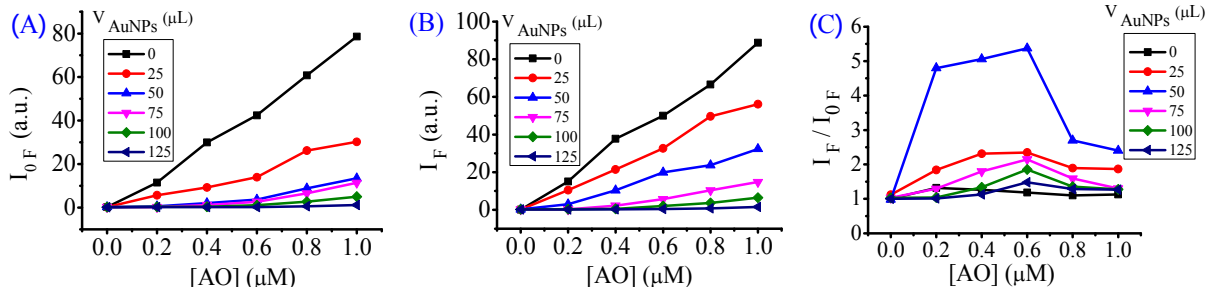

Fig. S3 Effects of AuNPs and AO concentrations on the fluorescence intensity of AO in the absence (A) and presence (B) of 2 μM Hg^{2+} in a Tris-HAc (10 mM, pH 7.0) buffer. (C) The emission enhancement of different concentrations of AO by 2 μM Hg^{2+}, where $I_{0\,F}$ and I_F are AO fluorescence intensities in the absence and presence of 2 μM Hg^{2+}, respectively. The excitation was at 490 nm, and the emission was recorded at 538 nm.

5. Effect of aptamer concentration

The concentration of aptamer affects the response behavior of the system for Hg^{2+}. Fig. S4 illustrates the change in fluorescence intensity of AO/T20/AuNPs (AO: 0.6 μM, AuNPs: 1.2 nM) upon the addition of different concentrations of T20 in the absence and presence of 2 μM Hg^{2+}. As a result, the mixture containing 100 nM T20 was optimized to obtain a better S/B.

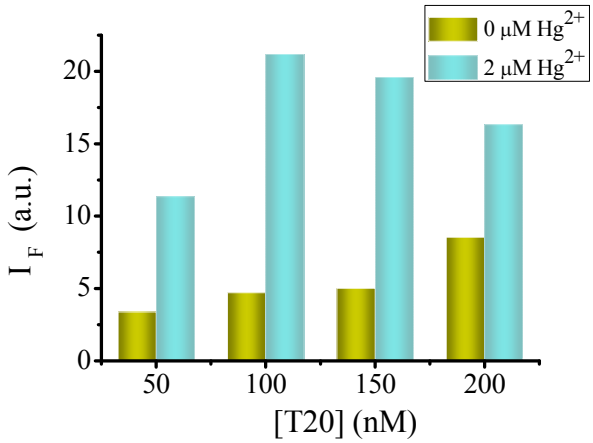

Fig. S4 The fluorescence intensity of AO/T20/AuNPs (AO: 0.6 μM, AuNPs: 1.2 nM) upon the addition of different concentrations of T20 (50 nM, 100 nM, 150 nM, 200 nM). Excitation and emission wavelengths were at 490 and 538 nm, respectively.

6. Effect of pH

Fig. S5 shows the effect of pH on the fluorescence intensity enhancement of AO by Hg^{2+} ions. The fluorescence intensity of AO is highly pH dependent. At relatively high pH values (pH > 9.0), the fluorescence of AO is very low. At a pH below 7.0, protonation of the nitrogen atoms of the thymine base reduces its affinity with Hg^{2+}. Fluorescence intensity ratio of the system ($I_F/I_{0\,F}$) increased with increasing pH, while decreased obviously when the pH is >7.0, where $I_{0\,F}$ and I_F are the AO fluorescence intensities in the absence and presence of Hg^{2+}, respectively. To get a high S/B, as well as a physiologically compatible condition, we chose Tris-HAc (pH 7.0) as the buffer system.

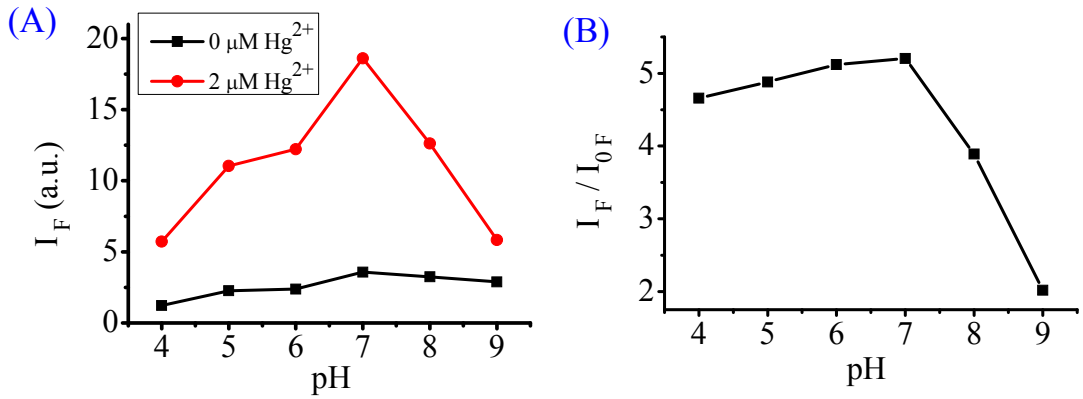

Fig. S5 (A) Effect of pH on the fluorescence intensity in the absence and presence of 2 μM Hg^{2+} in a Tris-HAc (10 mM, pH 7.0) buffer. (B) Fluorescence intensity ratio of AO/T_{20}/AuNPs (0.6 μM/100 nM/1.2 nM) as a function of pH, where $I_{0\,F}$ and I_F are the fluorescence intensities of AO at 538 nm in the absence and presence of 2.0 μM Hg^{2+}.

7. Effect of salt concentration

In addition, the sensitivity of the assay is influenced with the addition of salt. As can be seen in **Fig S6**, the fluorescence intensity increased with the addition of $NaNO_3$, while the colorimetric and RLS signals remarkably changed at 40 mM $NaNO_3$ solution. Different concentrations of NaCl also have been investigated. As shown in **Fig. S7** the NaCl induced optical signal changes were similar to those induced by $NaNO_3$.

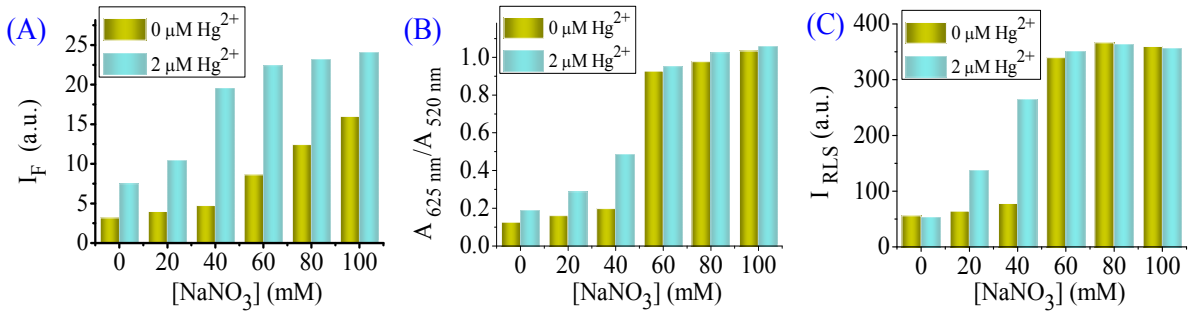

Fig. S6 Effects of ionic strength on the assay response. The (A) fluorescence intensity (538 nm), (B) absorption ratio ($A_{625\ nm}/A_{520\ nm}$), and (C) RLS intensity (645 nm) of AO/T20/AuNPs (0.6 μM/100 nM/1.2 nM) were measured in Tris-HAc (10 mM, pH 7.0) buffer solution containing different amounts of $NaNO_3$.

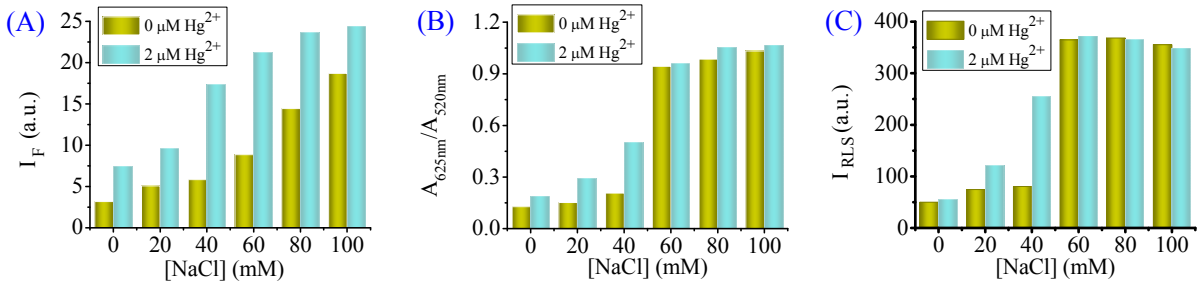

Fig. S7 Effect of NaCl on the assay response. The (A) fluorescence (538 nm), (B) absorption ratio ($A_{625\ nm}/A_{520\ nm}$) and (C) RLS (645 nm) of AO/T20/AuNPs (0.6 μM/100 nM/1.2 nM) were measured in Tris-HAc (10 mM, pH 7.0) buffer containing different amounts of NaCl.

8. The addition order of Hg^{2+}

Based on the principle of the detection method, there are three different analytical processes were designed. In strategy **1**, T20 and Hg^{2+} were first mixed and incubated for ~20 min, and then the AuNPs solution was added to the mixed solution and allowed to interact for ~1 h at room temperature. After that AO solution was mixed and incubated for another ~0.5 h at room temperature. In strategy **2**, T20 and AuNPs solution were first mixed and allowed to interact for ~1 h at room temperature, and then Hg^{2+} was added into the mixed solution and incubated for ~20 min. After that AO solution was mixed and incubated for another ~0.5 h at room temperature. In strategy **3**, T20 and AuNPs solution were first mixed and allowed to interact for ~1 h at room temperature, and then AO was added to the mixed solution and incubated at room temperature. 0.5 h later, Hg^{2+} was added to the mixed solution. The experimental results (see Fig. S8) showed that the sensitivity of the sensor in strategy 1 was the highest among the three strategies. Thus, we chose this addition strategy in the experiment.

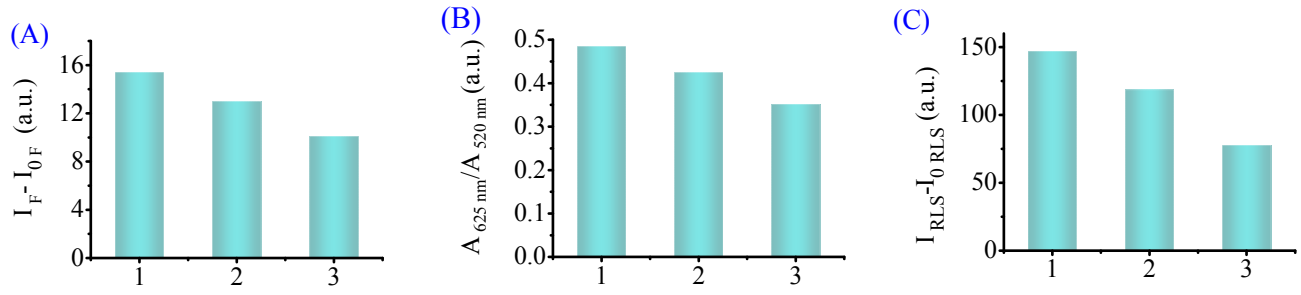

Fig. S8 Effects of different addition strategies on the detection of Hg^{2+}. The (A) fluorescence intensity (538 nm), (B) absorption ratio ($A_{625\,nm}/A_{520\,nm}$), and (C) RLS intensity (645 nm) of AO/T20/AuNPs (0.6 μM/100 nM/1.2 nM) were measured in Tris-HAc (10 mM, pH 7.0, 40 mM $NaNO_3$) buffer. (I_0 and I are the intensities in the absence and presence of 2.0 μM Hg^{2+}, respectively.)

9. The numbers of thymine repeat units

The length of the DNA strand would affect the sensitivity of our analytical system. Thus we used four different numbers of thymine repeat units (T10: poly-T_{10}, T15: poly-T_{15}, T20: poly-T_{20}, T35: poly-T_{35}) to test the hypothesis. Fig. S9A indicates that the longer DNA strand has a better ability to stabilize the AuNPs at the same $NaNO_3$ concentration. Fig. S9B also reveals that the aggregation of AuNPs is more sensitive toward Hg^{2+} in the presence of T20 than in the presence of T35. In this system, the aggregation extent directly influences the fluorescence intensity of AO (Fig. S9C). Based on these results, T20 was used in this experiment for the sensitive detection of Hg^{2+}.

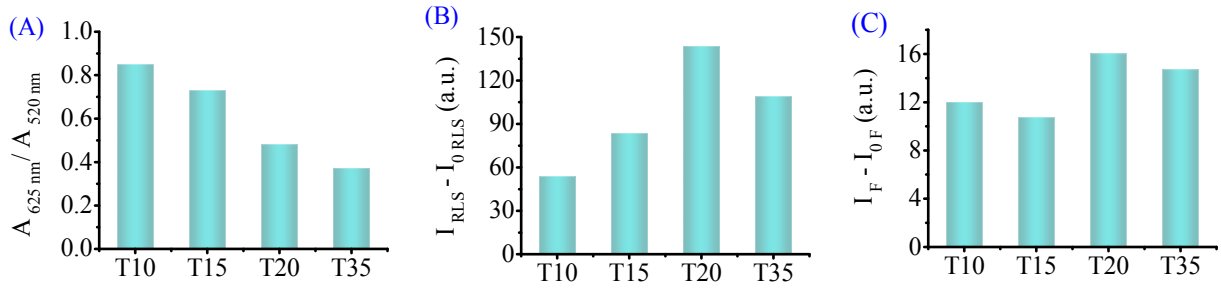

Fig. S9 Effects of different numbers of thymine repeat units on the detection of Hg^{2+}. The (A) absorption ratio ($A_{625\ nm}/A_{520\ nm}$), (B) RLS intensity (645 nm) and (C) fluorescence intensity (538 nm) of AO/T20/AuNPs (0.6 μM/100 nM/1.2 nM) were measured in Tris-HAc (10 mM, pH 7.0, 40 mM $NaNO_3$) buffer. (I_0 and I are the intensities in the absence and presence of 2.0 μM Hg^{2+}, respectively.)

10. Sensing kinetics of AO adsorbate upon addition of Hg^{2+}

Fig. S10 shows the sensing kinetics of AO adsorbate for different concentrations of Hg^{2+} to study the proper incubate time for the detection of Hg^{2+}. At first different concentrations of Hg^{2+} ions were incubated with T20/AuNPs at room temperature for ~1 h, and 0.6 μM AO was then added to the mixture before detection. The fluorescence intensity decreases at first, while about 30 min later it no longer gave an obvious change and kept stable in the next 30 min. These results indicated that the measurement of optical signals can be carried out 30 min later after the addition of AO to the Hg^{2+}/T20/AuNPs mixture solution

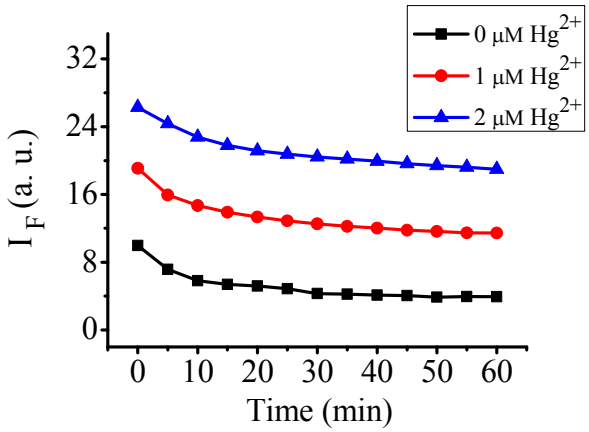

Fig. S10 Sensing kinetics of AO adsorbed on T20/AuNPs (AO: 0.6 μM, T20: 100 nM, AuNPs: 1.2 nM) upon addition of different concentrations of Hg^{2+} in the Tris-HAc (10 mM, pH 7.0) buffer. The excitation and emission wavelengths were at 490 and 538 nm, respectively.

11. UV–vis absorption spectra of AO/T20/AuNPs in the presence of different concentrations of Hg^{2+} ions

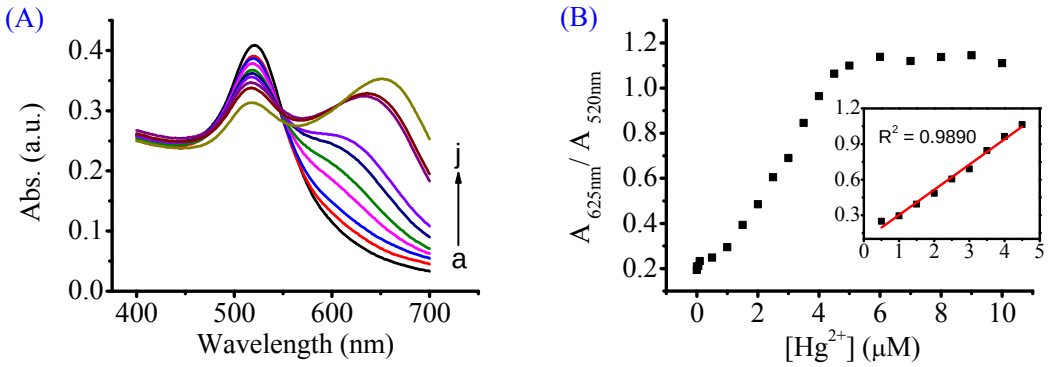

Fig. S11 (A)UV–vis absorption spectra of AO/T20/AuNPs (0.6 μM/100 nM/1.2 nM) in the presence of different concentrations of Hg^{2+} ions (from a to j (625 nm): 0, 0.5, 1.0, 1.5, 2.0, 2.5, 3.0, 3.5, 4.0, and 4.5 μM.) (B) Plot of absorption ratio ($A_{625\ nm}/A_{520\ nm}$) versus Hg^{2+} concentration. Inset is the calibration curve.

12. RLS spectra of AO/T20/AuNPs in the presence of different concentrations of Hg^{2+} ions

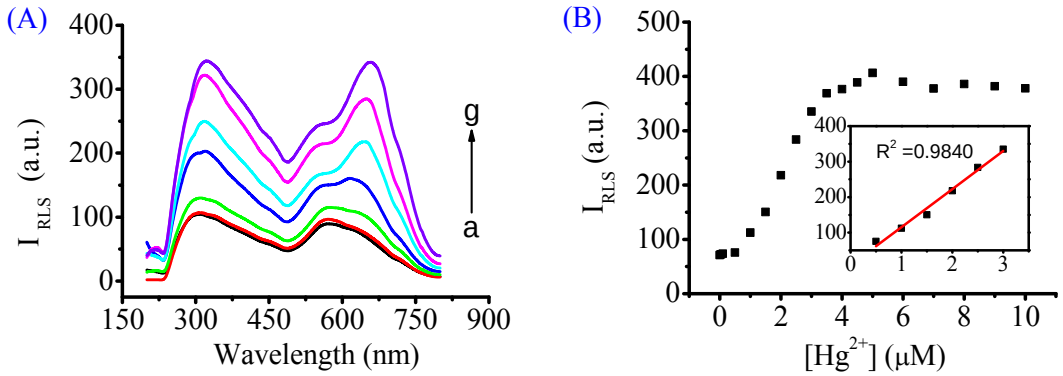

Fig. S12 (A) RLS spectra of AO/T20/AuNPs (0.6 μM/100 nM/1.2 nM) in the presence of different concentrations of Hg^{2+} ions (from a to g: 0, 0.5, 1.0, 1.5, 2.0, 2.5, and 3.0 μM). (B) Plot of RLS intensity (645nm) versus Hg^{2+} concentration. Inset is the calibration curve.

13. Comparison of this method with some other T-rich DNA based optical methods

Table S1 shows the comparison of this method for the detection of Hg^{2+} with some other T-rich DNA based optical methods. These results indicated that our proposed approach has a relatively high sensitivity for the detection of Hg^{2+}.

Table S1 Comparison of this method for the detection of Hg^{2+} with other optical methods.

Method	System	Linear range (nM)	Detection limit (nM)	Ref.
Fluorometry	F [a] and D [b] labeled T-rich DNA	40-100	40	**3**
	FAM [c] labeled T-rich DNA/SWNTs [d]	50-8000	14.5	**4**
	FAM labeled T-rich DNA/GO [e]	30-180	30	**5**
	T-rich DNA/Th T [f]	100-1200	20	**6**
Colorimetry	T-rich DNA/AuNPs [g]	500-5000	250	**7**
	T-rich DNA-functionlized AuNPs	100-2000	100	**8**
	T-rich DNAzyme/ H_2O_2 /CTAB [h]	10-1000	4.5	**9**
RS [i] assay	T-rich DNA/AuNPs	1.3-1667	0.7	**10**
	T-rich DNA/AuNPs/NH_2OH-Cu^{2+}	0.1-400	0.03	
This method	AO [j]/T-rich DNA/AuNPs	50-5000	30	**This method**

[a] F (fluorescein); [b] D (dabcyl); [c] FAM (carboxyfluorescein); [d] SWNTs (single-walled carbon nanotubes); [e] GO (graphene oxide); [f] Th T (thioflavine T); [g] AuNPs (gold nanoparticles); [h] CTAB (hexadecyl trimethyl ammonium bromide); [i] RS (resonance scattering) [j] AO (acridine orange).

14. The changes in the RLS and absorption signals of AO/T20/AuNPs that occurred by addition of some common metal ions

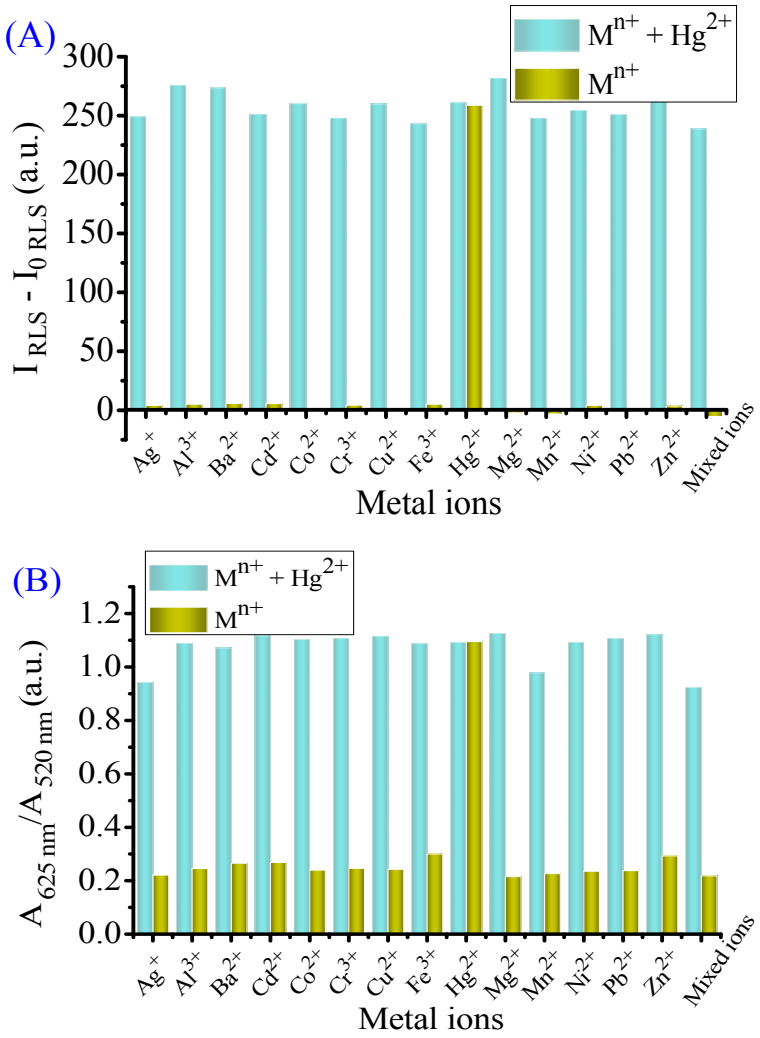

Fig. S13 (A) RLS intensity (645 nm) and (B) the absorption ratio ($A_{625\ nm}/A_{520\ nm}$) of AO/T20/AuNPs (0.6 μM/100 nM/1.2 nM) in 10 mM Tris-HAc buffer (40 mM $NaNO_3$, pH 7.0) in the presence of different metal ions. Concentration of Hg^{2+} is 5.0 μM and those of all other metal ions are 10.0 μM. (I_0 and I are the intensities in the absence and presence of metal ions, respectively.)

15. Detection of Hg^{2+} in tap water samples using the proposed method

The tap water sample was collected after discharging tap water for about 20 min and boiled for 5 min to remove chlorine.

Table S2. Detection of Hg^{2+} in tap water samples using the proposed method (n = 5).

Sample	Background content	Concentration		Recovery	RSD
	[nM]	Added [nM]	Found [nM]	[%]	[%]
Tap water 1	ND	100	94	94	3
Tap water 2	ND	200	207	104	3
Tap water 3	ND	300	289	96.3	4
Tap water 4	ND	400	388	97.0	3

ND: not detected

Supplementary references

1 K. C. Grabar, R. G. Freeman, M. B. Hommer and M. Natan, *J. Anal. Chem.*, 1995, **67,** 735–743.

2 W. Haiss, N. T. K. Thanh, J. Aveyard and D. G. Fernig, *Anal. Chem.*, 2007, **79,** 4215–4221.

3 A. Ono and H. Togashi, *Angew. Chem. Int. Ed.*, 2004, **43**, 4300–4302.

4 L. Zhang, T. Li, B. Li, J. Li and E. Wang, *Chem. Commun.*, 2010, **46**, 1476–1478.

5 S. He, B. Song, D. Li, C. Zhu, W. Qi, Y. Wen, L. Wang, S. Song, H. Fang and C. Fan, *Adv. Funct. Mater.*, 2010, **20**, 453–459.

6 Y. Wang, F. Geng, Q. Cheng, H. Xu and M. Xu, *Analyst*, 2011, **136**, 4284–4288.

7 C. W. Liu, Y. T. Hsieh, C. C. Huang, Z. H. Lin and H. T. Chang, *Chem. Commun.*, 2008, 2242–2244.

8 J. S. Lee, M. S. Han and C. A. Mirkin, *Angew. Chem. Int. Ed.* 2007, **46**, 4093–4096.

9 N. Lu, C. Shao and Z. Deng, *Analyst*, 2009, **134**, 1822–1825.

10 Z. Jiang, Y. Fan, M. Chen, A. Liang, X Liao, G. Wen, X. Shen, X. He, H. Pan and H. Jiang, *Anal. Chem.*, 2009**, 81**, 5439–5445.